Available online at www.sciencedirect.com
SCIENCE DIRECT®
Journal of Nuclear Materials 346 (2005) 56–65
journal of nuclear materials
www.elsevier.com/locate/jnucmat

# Spent fuel radionuclide source-term model for assessing spent fuel performance in geological disposal. Part I: Assessment of the instant release fraction

Lawrence Johnson [a,*], Cécile Ferry [b], Christophe Poinssot [b], Patrick Lovera [b]

[a] NAGRA, Wettingen, Switzerland
[b] CEA Saclay, Nuclear Energy Division, Department of Physics and Chemistry, BP.11, F-91191 Gif-sur-Yvette cedex, France

**Abstract**

A source-term model for the short-term release of radionuclides from spent nuclear fuel (SNF) has been developed. It provides quantitative estimates of the fraction of various radionuclides that are expected to be released rapidly (the instant release fraction, or IRF) when water contacts the $UO_2$ or MOX fuel after container breaching in a geological repository. The estimates are based on correlation of leaching data for radionuclides with fuel burnup and fission gas release. Extrapolation of the data to higher fuel burnup values is based on examination of data on fuel restructuring, such as rim development, and on fission gas release data, which permits bounding IRF values to be estimated assuming that radionuclide releases will be less than fission gas release. The consideration of long-term solid-state changes influencing the IRF prior to canister breaching is addressed by evaluating alpha self-irradiation enhanced diffusion, which may gradually increase the accumulation of fission products at grain boundaries.
© 2005 Elsevier B.V. All rights reserved.

*PACS:* 28.41.Kw

## 1. Introduction

The Spent Nuclear Fuel (SNF) source term in a water- saturated medium is normally described as the combination of two terms [1]:

- an instantaneous release of some radionuclides (RN) at the containment failure time, often referred to as the Instant Release Fraction (IRF), which represents the fraction of the inventory of safety-relevant radionuclides that may be rapidly released from the fuel and fuel assembly materials at the time of canister breaching;
- a slow long-term contribution corresponding to the dissolution of the uranium oxide matrix, given by a matrix alteration model.

This paper focuses on the IRF assessment for PWR fuels. Part II will focus on the matrix alteration model developed by CEA.

The IRF depends on the location of radionuclides in the rod after discharge from reactor and on its evolution

* Corresponding author. Tel.: +41 56 437 12 34; fax: +41 56 437 13 17.
*E-mail address:* lawrence.johnson@nagra.ch (L. Johnson).

0022-3115/$ - see front matter © 2005 Elsevier B.V. All rights reserved.
doi:10.1016/j.jnucmat.2005.04.071

with time before canister breaching. The locations of the preferentially released radionuclides after irradiation, their quantities and proposed estimates of the IRF for the key safety-relevant radionuclides are the subjects of the Sections 2–4 of this paper. The potential evolution of the IRF with time in an unbreached canister due to solid-state processes such as diffusion to grain boundaries or to free surfaces by alpha self-irradiation enhanced diffusion is briefly treated in the last paragraph. Various modeling approaches for estimating the IRF for PWR fuels are proposed here. Releases from the assembly materials and cladding are not quantitatively assessed here.

## 2. Overview of radionuclide distribution in fuel assemblies after discharge from reactor and of IRF various modeling approaches

During in-reactor irradiation, radionuclides produced in a nuclear fuel assembly may stay in the locations in which they are produced or may migrate due to various mechanisms, including recoil, diffusion, grain growth and rim restructuring. An overview of the main fuel assembly components, the nuclides of interest and the expected locations of nuclides upon discharge of the fuel from the reactor is given in Table 1, based on a number of studies [2–5]. The degree of segregation of

Table 1
Expected distributions of radionuclides in fuel assemblies and possible modeling approaches

| Components | Key radionuclides | Characteristics and possible modeling approach |
|---|---|---|
| *Fuel assembly structural materials* | | |
| Zirconia | $^{14}C$ (organic?) | Oxide film typically about 40–80 μm thick is formed in reactor (about 10% of cladding thickness).The oxide has a low solubility; the outer part is porous and; may incorporate nuclides present in Zircaloy as the film grows. *Limited data on Zircaloy indicating preferential release; consider* $^{14}C$ *as part of IRF. No data on stainless steels* |
| Zircaloy, Inconel and steel | $^{14}C$ (organic?), $^{36}Cl$, $^{59}Ni$, $^{63}Ni$ | Very low general corrosion rate. *Release of all nuclides plus remaining* $^{14}C$ *congruent with the slow corrosion rate* |
| *Uranium oxide fuel* | | |
| Gap | Fission gases, volatiles ($^{139}I$, $^{137}Cs$, $^{135}Cs$, $^{36}Cl$, $^{79}Se$, $^{126}Sn$ (?)). Also $^{14}C$ (non-volatile but partially segregated) | Good data for some nuclides. Assessment through fission gas release measurements and correlation with leaching experiments. *Part of IRF* |
| Rim porosity | Fission gases, volatiles ($^{129}I$, $^{137}Cs$, $^{135}Cs$, $^{36}Cl$, $^{79}Se$, $^{126}Sn$ (?)) | Rim width a function of burnup; good data available. Large proportion of nuclides in rim region segregated into pores and secondary phases during restructuring. No experimental data indicating release. *Pessimistically could be part of the IRF; alternatively, may be treated separately* |
| Rim grains | Actinides, FP | Release through dissolution when water arrives. FP may also diffuse to rim pores by αSIED. *FP inventory may thus be part of IRF or MAM* |
| Grain boundaries | Fission gases, volatiles ($^{129}I$, $^{137}Cs$, $^{135}Cs$, $^{36}Cl$, $^{79}Se$, $^{126}Sn$(?)) and segregated metals ($^{99}Tc$, $^{107}Pd$) | Limited data. *As for rim pores, pessimistically considered part of IRF, alternatively could be treated separately* |
| Grains | Actinides, remaining FP and activation products | Belongs to MAM |
| *MOX fuel* | | |
| Gap | As for $UO_2$ | Assessment through fission gas release only. Little leaching data. *Part of IRF* |
| Grain boundaries and porosity in $PuO_2$ grains | As for $UO_2$ | Assessment through fission gas porosity characterisation. *Conservatively considered part of IRF* (see Section 4) |
| Grains | As for $UO_2$ | Belongs to MAM |

the various radionuclides is highly dependent on fuel operating parameters such as linear power rating and burnup, as discussed in the next section.

Table 1 suggests that the definition of what should be included in the IRF is subject to considerable uncertainty and acknowledges subjective assessments regarding likelihood of processes (e.g. leaching of the inventory present at the grain boundaries). The following approaches and definitions are adopted in this paper:

- best estimate (BE) – one based on a good understanding of the mechanism and a good quality database (e.g. fission gas release in moderate burnup $UO_2$ fuel and rim restructuring in moderate to high burnup $UO_2$ fuel);
- bounding or pessimistic estimate (PE) – an estimate based on data and process understanding that provides a maximum for the range of derived values; this is expected to result in overprediction of average IRF values; here this applies particularly to cases where data is extremely limited or unavailable, thus understanding of the processes or of chemical analogues must be used to derive estimates.

The approach taken is to develop BE IRF values for moderate burnup $UO_2$ fuel for nuclides for which data exists ($^{137}Cs$ and $^{129}I$), because it is judged that the understanding and data are sufficient to support this, and to derive only pessimistic estimate (PE) IRF values for radionuclides for which little data is available and in the case of MOX fuel and higher burnup $UO_2$ fuel.

Radionuclide distributions in spent nuclear fuel rods as a function of fuel burnup are based on fission gas release data as a function of the burnup and type of fuel (see Section 3) and on leaching data giving radionuclide inventories in the gap and grain boundaries as a function of fission gas release (see Section 4). In high burnup $UO_2$ fuel and MOX fuel, behavior of radionuclides based on fission gas release in the restructured zone of the rod must also be taken into account.

## 3. Fission gas distribution in PWR fuel

### 3.1. $UO_2$ fuel fission gas release and rim restructuring

#### 3.1.1. Fission gas release (FGR)

The release of fission gas from $UO_2$ fuel is strongly correlated with the linear heat rating, which is dependent on fuel temperature [6]. Optimization of fuel assembly designs and irradiation conditions help to ensure that linear heat ratings are kept low and thus FGR is minimized [7]. As a result, FGR values are typically <1% at burnups below 40 GWd $t^{-1}_{iHM}$, as shown in Fig. 1. At higher burnups, a reduction of thermal conductivity increases the fuel temperatures, thus FGR tends to increase [8].

#### 3.1.2. Fission gas behavior in high burnup $UO_2$ fuel and rim restructuring

In high burnup $UO_2$ fuel (>40 GWd $t^{-1}_{iHM}$), a restructured region appears around the periphery of the $UO_2$ pellet due to the high local burnup. The rim region is characterized by small grains (around 0.5 μm) and large closed porosity (10%–15%) filled with over-pressured fission gas bubbles of micrometre size [3].

Characteristics of the rim zone, such as rim thickness and fission gas content as a function of burnup, have been studied by Koo et al. [9] based on a literature review. From the analysis of this data, the mean local burnup within the entire rim region is 1.33 times the average pellet burnup, which is consistent with local neodymium profile measurements. As illustrated in Fig. 2, the best estimate of the rim thickness at an average burnup of 50 GWd $t^{-1}_{iHM}$ is 50 μm, increasing to 120 μm and

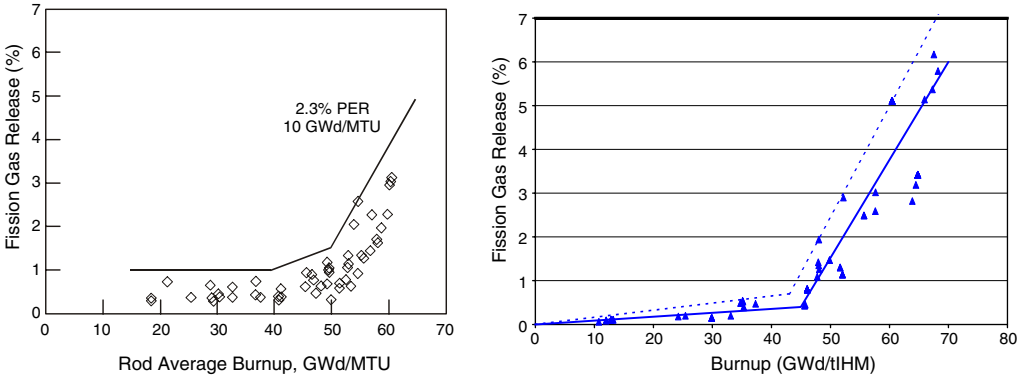


Fig. 1. Fission gas release from PWR fuel as a function of burnup (left) from [7] the line represents the the bounding values of all data (right) from CEA data, solid line – best fit; dashed line – bounding or pessimistic estimate.

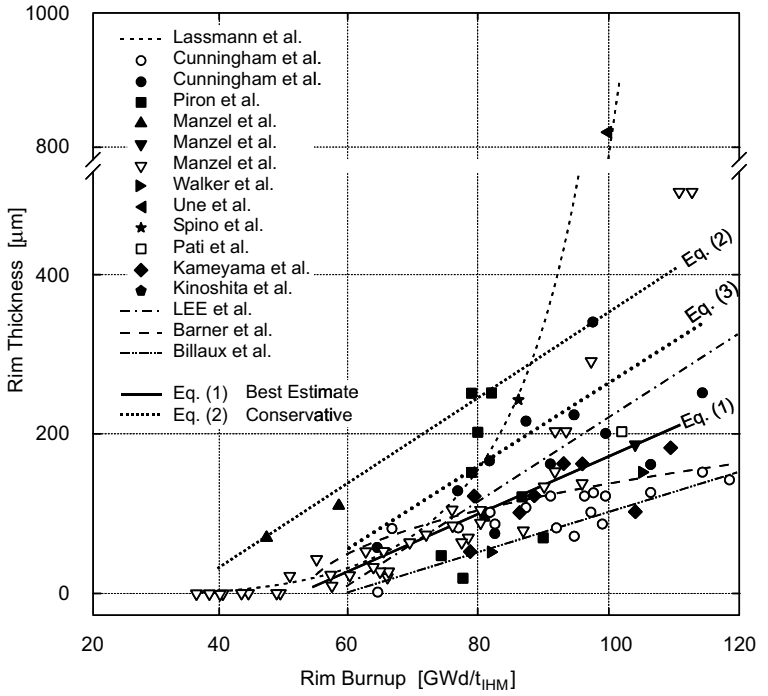


Fig. 2. Rim width in μm as a function of burnup (GWd/$t_U$), from [9]. Eq. (1) represents a best fit of the data, while Eq. (2) is a 'conservative' or pessimistic expression that encompasses almost all the data proposed by Koo et al. Eq. (3) is the pessimistic expression proposed here. The references are in the original paper [9].

170 μm at 65 and 75 GWd $t_{iHM}^{-1}$ using a best fit (Eq. (1) in [9]) of all the data. This best fit is represented by

$$R_t = 3.55BU_R - 185, \quad (1)$$

where $R_t$ is the rim thickness (μm) and $BU_R$ is the rim burnup (GWd $t_{iHM}^{-1}$). A pessimistic function that bounds all the data is also given in [9] by

$$R_t = 5.28BU_R - 178. \quad (2)$$

However, use of the latter expression suggests that significant rim thicknesses exist even in fuels with burnups in the range of 30 GWd $t_{iHM}^{-1}$. Because this seems completely inconsistent with microstructural studies, a revised expression was developed, given by:

$$R_t = 5.44BU_R - 281. \quad (3)$$

This expression gives no rim below 40 GWd $t_{iHM}^{-1}$ and is still pessimistic with respect to almost all data points in Fig. 2.

Koo et al. [9] combine Eqs. (1) and (2) with an expression for the Xe distribution in the fuel to calculate the fraction of the total Xe produced in the pellet that is retained in the rim pores assuming no release to the gap during restructuring (Fig. 4 in the original paper). The fraction of the fission gases produced that is present in rim pores for various burnups of $UO_2$ fuel, based on Fig. 4 of [9], with revision of the 'conservative' curve according to application of Eq. (3) rather than Eq. (2), is summarised in Table 2. Also given are the values for

Table 2
Fraction of the total fission gas (FG) inventory in a fuel rod that is present in the pores in the rim region of $UO_2$ fuel with burnups of 37, 41, 48, 60 and 75 GWd $t_{iHM}^{-1}$, based on Eqs. (1) (BE) and (3) (PE). The fraction of fission gas present in the rim region (pores plus grains) is also given

| Average burnup (GWd $t_{iHM}^{-1}$) | Rim burnup (GWd $t_{iHM}^{-1}$) | % of total FG present in the rim pores in (BE) | % of total FG present in the rim pores (PE) | % of total FG present in the rim (pores + grains) (BE) | % of total FG present in the rim (pores + grains) (PE) |
|---|---|---|---|---|---|
| 37 | 49 | 0 | 0 | 0 | 0 |
| 41 | 55 | 0 | 0.5 | 0.7 | 1.25 |
| 48 | 64 | 2 | 3 | 2.7 | 4.3 |
| 60 | 80 | 4 | 8 | 6.3 | 9.8 |
| 75 | 100 | 8 | 14 | 10.8 | 16.5 |

the percentage of total FG inventory in the fuel that is found within the rim region (pores plus grains) based on a simple calculation of the fractional volume of the rim with a correction for the 1.33 times higher average burnup in the rim. This illustrates clearly that most of the fission gas produced in the rim is present in pores (about 70%–80%).

In spite of the high degree of restructuring of the rim, fission gas is retained in the new pore structure [9], which explains the low overall fission gas release for PWR fuels at high burnups (Fig. 1). Nonetheless, the fission gas in this region can be considered released from the fuel matrix, even though it is not released to the void space in the fuel rod. Similarly, other fission products that are not in solid solution in $UO_2$ can be expected to be released from the grains during restructuring. As a result, from the perspective of release under disposal conditions, such fission products can be considered to belong to the grain boundary inventory of the fuel and be potentially available for release if groundwater penetrates grain boundaries.

For the radionuclide release model, options for treating the fission products present within the grains are to consider them as part of the IRF because of the small grain diameter or to consider them being released more slowly by matrix dissolution.

### 3.2. MOX Fuel-fission gas release and restructuring

#### 3.2.1. Fission gas release

The irradiation of MOX fuel on a routine basis in commercial power reactors began in the late 1980s. As a result, compared to FGR data for $UO_2$ fuels, data for MOX fuel is somewhat limited. The data from CEA post-irradiation examinations are shown in Fig. 3. FGR for MOX PWR fuel rods increases rapidly above 40 GWd $t_{iHM}^{-1}$. The limited data above 45 GWd $t_{iHM}^{-1}$ suggests that the FGR reaches about 5% at 50 GWd $t_{iHM}^{-1}$ and approaches 10% at 70 GWd $t_{iHM}^{-1}$. Increased FGR relative to $UO_2$ fuel at higher burnups arises from higher reactivity and higher power/temperatures compared with $UO_2$ fuel, as well as microstructural factors (see Table 3).

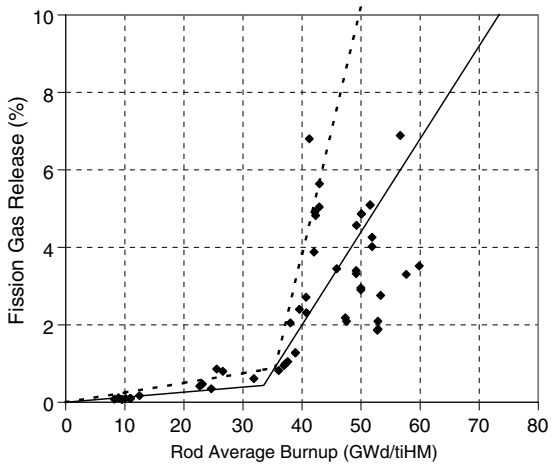


Fig. 3. FGR measured in MOX fuels after irradiation, solid line – best fit; dashed line – bounding or pessimistic estimate.

Table 3
Microstructural features of a MOX (Ammonium Di-Uranate powders) type $UO_2$ powders [10]

| | Pu-rich agglomerates | Coating phase | Phase '$UO_2$' |
|---|---|---|---|
| Surface fraction (%) | 11.1 | 42.2 | 46.7 |
| Plutonium fraction (%) | 38.5 | 46.3 | 15.2 |
| Average Pu concentration % ahm[a] | 20.2 | 7.3 | 2.7 |

[a] Atoms heavy metal.

#### 3.2.2. Restructuring in MOX fuel

The Pu-rich agglomerates in MOX fuel, which have a diameter larger than ~10 μm, experience a burnup which is much higher than the rest of the fuel, resulting in a structure analogous to that of the rim from the mid-radius of the pellet, as illustrated in Fig. 4.

Assuming that large Pu-rich agglomerates, which represent ~11% of the overall surface (see Table 3 [10]), have an average burnup which is ~3 times higher than the average pellet burnup [3], fission products present in the large restructured Pu-rich agglomerates represent around 25% of the overall inventory.[1] This value, obtained on the basis of surface distribution of large agglomerates, is in agreement with intergranular gas fraction present essentially in the Pu-rich restructured agglomerates undetected by microprobe (CEA data) and with the gas release observed during experiments of thermal annealing. Thus most of the gas created is found in aggregate porosity. The quantities of fission gas in the gap and pores of large Pu-rich agglomerates are summarised in Table 4. A pessimistic estimate is proposed based on the total activity contained in all Pu agglomerates (pores plus grains) located in the external part of the pellet from the mid-radius whatever their size. These evaluations are dependent on the fabrication method (heterogeneous MOX fuels).

[1] Proportion of agglomerates in the external zone × surface fraction × average local fission yield.

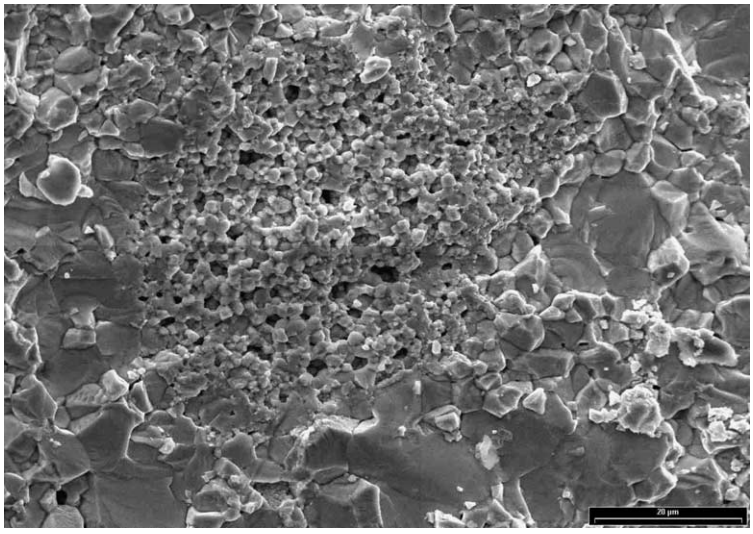

Fig. 4. Electron micrograph of MOX fuel, showing the restructuring and high fission gas porosity in a $PuO_2$ grain, surrounded by grains of $UO_2$ with low burnup and little porosity (CEA data).

Table 4
Distribution of the fission gas in MOX fuel for various burnups (BU); best estimate and pessimistic values

| BU (GWd $t_{iHM}^{-1}$) (%) | | 40 | 45 | 55 | 60 |
|---|---|---|---|---|---|
| Gap | Average | 2 | 3.2 | 5.6 | 6.8 |
| | Pessimistic | 3.8 | 7.0 | 13.4 | 16.6 |
| Restructured Pu-rich agglomerates | Average | 25 | 30 | 30 | 35 |
| | Pessimistic | 50 | 50 | 50 | 50 |
| Gap + restructured Pu-rich agglomerates | Average | 27 | 33 | 36 | 42 |
| | Pessimistic | 54 | 57 | 63 | 67 |

## 4. Leaching of radionuclides from spent fuel and estimated IRF values

### 4.1. Leaching data

Although the total number of fuel rods studied to determine the quantities of radionuclides in the gap and at grain boundaries are small, it is nonetheless possible to estimate average values because gap and grain boundary inventories can be correlated with FGR for individual fuel rods and because FGR can be reliably estimated for burnups up to about 65 GWd $t_{iHM}^{-1}$ for PWR fuel. This approach has been used in Canadian [11] and Swedish [2] assessment studies for CANDU (Canada deuterium uranium) and BWR (boiling water reactor) fuels, respectively.

The relationship between FGR and leaching of a number of fission products from $UO_2$ fuel has been reviewed recently [2,4]. In the present study, additional data from the CEA program have been added to the database, as shown in Table 5. The data on FGR from ATM-106 PWR fuel for a burnup of 50 GWd $t_{iHM}^{-1}$ lie far above the range of values in Fig. 1. Although this result is highly atypical, the data are nonetheless retained in the present study because of the importance of the associated results on fission product leaching. CANDU fuel data provides much of the basis for the $^{14}C$ IRF estimates in the present study and provides the only $^{36}Cl$ leaching data available for spent fuel [2]. For $^{14}C$, the IRF has been shown to be unrelated to FGR [2]. A further important observation is the absence of any leaching data for fuel with burnup exceeding 50 GWd $t_{iHM}^{-1}$ and the rare data for MOX fuel.

For many of the radionuclides for which leaching measurements are not available, the only basis for the estimates are the observations that diffusion coefficients in $UO_2$ during reactor irradiation decreases in the order I > Cs > other fission products, and the understanding of fission product chemistry, which has identified which fission products form solid solutions with $UO_2$ and which form secondary phases [21]. An indication that using Cs or I to bound the release of other fission products is a conservative approach can be obtained by considering the case of Cd, one the most volatile of the fission products (after FG, Cs and I) [22]. Quantitative X-ray photoelectron spectroscopy of grain boundaries in CANDU fuel has been reported in [23], in which it is noted that Cd was only occasionally detected and would have been routinely seen if it had experienced the same fractional release as Cs. Iodine was not observed perhaps because of its low fission yield. The IRF for $^{129}I$ should thus provide a bounding value which would not be exceeded by other fission products.

Table 5
Gap and grain boundary (GB) leaching data for PWR $UO_2$ fuels

| Fuel I.D. | Burnup (GWd $t_{iHM}^{-1}$) | FGR (%) | Cs Gap (%) | Cs GB (%) | Sr Gap (%) | Sr GB (%) | Tc Gap (%) | Tc GB (%) | I Gap (%) | I GB (%) | C Gap (%) |
|---|---|---|---|---|---|---|---|---|---|---|---|
| PWR (Ringhals)[a] | 43 | 1.05 | ~1 | | | | | | | | |
| ATM-103[b] (PWR) | 30 | 0.25 | 0.2 | 0.48 | 0.01 | 0.11 | | | | | |
| ATM-104[b] (PWR) | 44 | 1.1 | 1.2 | 0.1 | | | | | | | |
| ATM-106[b] (PWR) | 43 | 7.4 | 2 | 0.5 | 0.11 | 0.03 | 0.13 | | 0.1 | 8.5 | |
| ATM-106[b] (PWR) | 46 | 11.0 | 2.5 | 1.0 | 0.02 | 0.13 | 0.01 | 0.01 | 1.2 | 8.0 | |
| ATM-106[b] (PWR) | 50 | 18.0 | 6.5 | 1.0 | 0.1 | 0.07 | 0.05 | 0.12 | 15 | 7.6 | |
| CEA (PWR) | 22 | 0.1 | 0.3 | | | | | | | | |
| CEA (PWR) | 37 | 0.2 | 0.6 | | | | | | | | |
| CEA (PWR) | 47 | 0.5 | 2.3 | | | | | | | | |
| CEA (PWR) | 60 | 2.8 | 1.0 | | | | | | | | |
| PWR–HBR[c] | 31 | 0.2 | 0.8 | | 0.024 | | 0.03 | | 0.008 | | 0.001 |
| PWR–TP[c] | 27 | 0.3 | 0.32 | | 0.012 | | 0.04 | | 0.002 | | |
| PWR–HBR[d] | 31 | 0.2 | | | | | | | 0.284 | | 0.33 |
| PWR–TP[d] | 27 | 0.3 | 0.4 | | | | <0.01 | | 0.076 | | 3.0 |
| ATM-101[e] (PWR) | 28 | 0.2 | 2 | | | | | | 4 | | 2–7 |
| MOX[f] | 12–25 | Not reported | 10–12 | | | | | | 1 to 2 | | |
| CEA–MOX | 47 | 7 | 3.2 | | | | | | | | |

[a] Refs. [12,13].
[b] Ref. [14]: data are estimated from graph as raw data are not presented. Data represent average values of repeat measurements.
[c] Ref. [15,16]: data at 25 °C.
[d] Refs. [17,18]: data at 85 °C.
[e] Ref. [19]: crushed fuel, includes grain boundary inventory; data at 200 °C for 9 months, results likely represent IRF plus some matrix dissolution.
[f] Ref. [20].

There is some doubt whether Pd and Tc should be included in the category of nuclides with a significant IRF, as these elements are present in $UO_2$ as insoluble alloy inclusions, thus releases are extremely small, as noted in leaching studies [2]. Nonetheless, because they segregate significantly to grain boundaries, values are assigned here based on the extent of restructuring in the rim region. The very different aqueous chemistry of the various nuclides segregated from the matrix plays an important role in determining the actual release to solution, in that some elements are highly soluble (I, Cs) and others may be relatively insoluble and resistant to dissolution. This aspect is not addressed in the IRF model, which is focused on estimating the amounts segregated. As a result the quantities of the latter that are actually released may have to be assessed through other approaches, such as kinetic studies or solubility estimates.

### 4.2. Estimated IRF values for $UO_2$ fuel at $t = 0$

The estimated gap and grain boundary (GB) inventories for important radionuclides are listed in Table 6 for PWR $UO_2$ fuels with burnups of 37, 41, 48, 60 and 75 GWd $t_{iHM}^{-1}$. All other radionuclides are assumed to be homogeneously distributed in the fuel matrix. The approach in developing the estimates has been to use best estimate (BE) correlations of Cs and I release with FGR to estimate the gap values for all burnups. GB inventories for Cs and I are based on BE values up to 48 GWd $t_{iHM}^{-1}$, including the rim porosity values given in Table 2. Rather pessimistic values for $^{14}C$ and $^{36}Cl$ are adopted because of the very limited data and understanding of release behavior for these nuclides. For Se and Sn, the experiments of Wilson [24] suggest that there is likely only a small release to the gap [4]. For higher burnups, the fission gas release is used to bound the gap release of volatile and semi-volatile radionuclides. The GB releases at high burnups are based on the pessimistic estimate values for rim porosity given in Table 2.

An optional approach is to assume pessimistically that water penetrates all pores rapidly. This leads to the IRF values (i.e. gap and GB combined) in Table 7.

### 4.3. Estimated IRF values for MOX fuels at $t = 0$

Regarding values presented in Table 4 for fission gas segregation in MOX fuel, the lack of leaching data and the lack of knowledge concerning the long-term evolution of very porous zones as the Pu-rich agglomerates (as the rim zone in $UO_2$ fuels (see Section 3.1) makes it difficult today to propose IRF values for MOX fuels.

It is clear that, once exposed to water, such porous regions are likely to be susceptible to rapid leaching of fission products present in the pores. The assumption

Table 6
Gap and GB inventory estimates (% of total inventory) for various radionuclides for PWR $UO_2$ fuel, based on BE values for burnups of 48 GWd $t_{iHM}^{-1}$ or less and PE values for higher burnups

| BURNUP | 37 | | 41 | | 48 | | 60 | | 75 | |
|---|---|---|---|---|---|---|---|---|---|---|
| RN | Gap | GB | Gap | GB | Gap | GB | Gap | GB | Gap | GB |
| Fission gas | 1 | 1 | 1 | 1 | 1 | 3 | 4 | 8 | 8 | 14 |
| $^{14}C^{*}$ | 10 | | 10 | | 10 | | 10 | | 10 | |
| $^{36}Cl$ | 5 | | 5 | | 10 | | 12 | | 25 | |
| $^{79}Se$ | 0.1 | 1 | 0.1 | 1 | 0.1 | 2 | 0.4 | 8 | 0.8 | 14 |
| $^{90}Sr$ | 1 | – | 1 | – | 1 | – | 1 | 8 | 1 | 14 |
| $^{99}Tc$ | 0 | 1 | 0 | 1 | 0 | 2 | 0 | 8 | 0 | 14 |
| $^{107}Pd$ | 0 | 1 | 0 | 1 | 0 | 2 | 0 | 8 | 0 | 14 |
| $^{126}Sn$ | <0.01 | 1 | <0.01 | 1 | <0.01 | 2 | <0.01 | 8 | <0.01 | 14 |
| $^{129}I$ | 1 | 2 | 1 | 2 | 1 | 3 | 4 | 8 | 8 | 14 |
| $^{135}Cs$ | 1 | 1 | 1 | 1 | 1.5 | 1 | 4 | 8 | 8 | 14 |
| $^{137}Cs$ | 1 | 1 | 1 | 1 | 1.5 | 1 | 4 | 8 | 8 | 14 |

Table 7
IRF estimates (% of total inventory) for various radionuclides for PWR $UO_2$fuel, assuming IRF comprises gap, grain boundaries and all fission products in rim region (grains plus pores). BE values, with PE values in brackets

| BURNUP | 37 | 41 | 48 | 60 | 75 |
|---|---|---|---|---|---|
| RN | IRF | IRF | IRF | IRF | IRF |
| Fission gas | 2 (2) | 2 (3) | 4 (6) | 10 (16) | 18 (26) |
| $^{14}C^{*}$ | 10 | 10 | 10 | 10 | 10 |
| $^{36}Cl$ | 5 | 5 | 10 | 16 | 26 |
| $^{79}Se$ | 1 (1) | 1 (2) | 3 (4) | 7 (11) | 11 (17) |
| $^{90}Sr$ | 1 (1) | 1 (2) | 3 (4) | 7 (11) | 11 (17) |
| $^{99}Tc$ | 1 (1) | 1 (2) | 3 (4) | 7 (11) | 11 (17) |
| $^{107}Pd$ | 1 (1) | 1 (2) | 3 (4) | 7 (11) | 11 (17) |
| $^{126}Sn$ | 1 (1) | 1 (2) | 3 (4) | 7 (11) | 11 (17) |
| $^{129}I$ | 3 (3) | 3 (3) | 4 (6) | 10 (16) | 18 (26) |
| $^{135}Cs$ | 2 (2) | 2 (2) | 4 (6) | 10 (16) | 18 (26) |
| $^{137}Cs$ | 2 (2) | 2 (2) | 4 (6) | 10 (16) | 18 (26) |

that the fission product inventory in the agglomerates should be part of the IRF is clearly very conservative, as this inventory should not be accessible to water when the fuel cladding is breached, because the agglomerates are surrounded and isolated by grains of dense low porosity $UO_2$. Nonetheless, there is today no data for MOX fuels to argue that a part of grain boundaries and pores will not open, possibly even before breaching of confinement.

## 5. Contribution of alpha self-irradiation enhanced diffusion to the IRF

A release of radionuclides from the grains to grain boundaries or to the free surface of the fuel before the canister breaching should increase the IRF. It has been demonstrated that classical thermal diffusion is not relevant at the temperature and over time of disposal [25]. However, given that radiation-enhanced diffusion is observed in reactor due to fission fragment effects, a mechanism of diffusion due to alpha self-irradiation is expected to occur under repository conditions. Theoretical approaches have been developed in order to evaluate the diffusion coefficient induced by alpha self-irradiation (see paper of Ferry et al., this issue). They show that uncertainties of up to three orders of magnitude exist concerning the value of the alpha self-irradiation diffusion coefficient.

Most of the fission gas in the rim is segregated to the pores after rim restructuring (about 85% at a rim burnup of 80 GWd $t_{iHM}^{-1}$). Because the estimates in Table 1 accounting for the rim fraction are already rather pessimistic given the 'bounding' approach, the alpha enhanced diffusional loss calculation is not applied to this region.

The cumulative fraction of RN released from the grains of the core of the pellet as a function of time

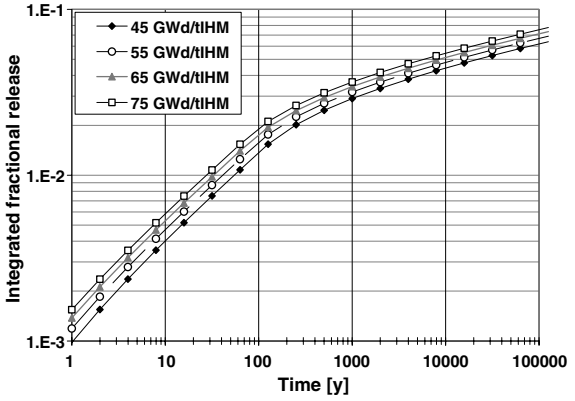


Fig. 5. Calculated released fraction from grains due to α self-irradiation enhanced diffusion for $UO_2$ fuels with burnups of 45, 55, 65 and 75 GWd $t_{iHM}^{-1}$ [5].

was calculated from Booth's model [26] assuming grains as spheres of 8 μm and grain-boundaries as perfect sinks. The upper estimate of the diffusion coefficient $D_\alpha^*$ ($m^2 s^{-1}$) as a function of the volume alpha activity of the spent fuel $A_\alpha$ ($Bq\,m^{-3}$) given by:

$$D_\alpha^*(t) = 2 \times 10^{-41} A_\alpha(t), \quad (4)$$

was used for the calculation.

Fig. 5 shows the fraction released in grain boundaries as a function of time and burnup in $UO_2$ fuels. Thus with these pessimistic assumptions, after 10000 years of disposal, the fraction released from the grains is close to 5% whatever the fuel burnup. It indicates a limited effect of the alpha enhanced diffusion contribution although an upper estimate of $D_\alpha^*$ was used in the calculation.

## 6. Conclusions

Results from studies of fission product leaching from spent fuel performed over the past 20 years have been evaluated in the context of information from investigations of FGR and fuel restructuring as a function of burnup, to provide a basis for estimating the instant release fraction (IRF) of radionuclides that will be released under geological disposal conditions. Different approaches for assessing the IRF that reflect greater or lesser degrees of pessimism have been proposed in the paper. These approaches depend on the leaching data available in literature and on the anticipated long-term evolution of the spent fuel pellet microstructure before breaching of confinement.

The results permit reliable IRF estimates to be made for several important long-lived radionuclides (e.g $^{129}I$ and $^{135}Cs$) for moderate burnup $UO_2$ fuel and bounding estimates to be made for high burnup $UO_2$ fuel. The results suggest relatively low IRF values for low to moderate burnup fuel and potentially high IRF values for high burnup fuel in which higher FGR and significant fuel restructuring occurs.

For high burnup $UO_2$ fuel and MOX fuel, the leaching data are extremely limited. Further studies of fission product leaching for such fuels are clearly warranted. Furthermore, for such fuels, IRF values depend significantly on the degree of contribution of the inventory potentially present in pores of the restructured zones (rim or Pu-rich clusters). Improvement of pessimistic IRF values requires determination of the time evolution of the open porosity in the spent fuel rod before breaching of confinement.

## Acknowledgements

The authors thank Dr Christophe Jegou providing the CEA leaching data.

This work has been supported by the European Commission through a European cofunded project entitled SFS (FIKW-CT-2001-00192 SFS) and partially by the French Electricity Utility EDF.

## References

[1] L.H. Johnson, N.C. Garisto, S. Stroes-Gascoyne, Proc. Waste Manage. 1985 (1985) 479.
[2] L.H. Johnson, J.C. Tait, Release of segregated radionuclides from spent fuel, SKB Technical Report 97–18 (1997).
[3] Poinssot, C.P. Toulhoat, J-P. Grouiller, J. Pavageau, J-P. Piron, M. Pelletier, P. Dehaudt, C. Capellaere, R. Limon, L. Desgranges, C-Jegou, C. Corbel, S. Maillard, M-H. Fauré, J-C. Cicariello, M. Masson, Synthesis on the long-term behavior of the spent nuclear fuel, Vol. 1. CEA Report CEA-R-5958(E) (2001), p. 304.
[4] L.H. Johnson, C. Poinssot, C. Ferry, P. Lovera, Estimates of the instant release fraction for $UO_2$ and MOX fuel at $t = 0$, Nagra Technical Report NTB 04-08 (2004).
[5] C. Ferry, P. Lovera, C. Poinssot, L. Johnson, in: Oversby, Werme (Eds.), Scientific Basis for Nuclear Waste Management XXVII Mater. Res. Soc. Symp. Proc. 807 (2003), p. 35.
[6] K. Kamimura, in: Proceedings of the Technical Committee Meeting on Fission Gas Release and Fuel Rod Chemistry Related to Extended Burnup, Pembroke, Ont., Canada, 28 April–1 May 1992, IAEA-TECDOC-697 (1992), p. 82.
[7] G. Vesterlund, L.V. Corsetti, in: Proceedings of the 1994 International Topical Meeting on Light Water Reactor Fuel Performance, West Palm Beach, Florida, 17–21 April, p. 62.
[8] J. Spino, in: Advances in Fuel Pellet Technology for Improved Performance at High Burnup, IAEA-TECDOC-1036 (1998), Proceedings of the Technical Committee Meeting, Tokyo, 28 October–1 November, 1996, IAEA, Vienna.
[9] Y.-H. Koo, B.-H. Lee, J.-S. Cheon, D.-S. Sohn, J. Nucl. Mater. 295 (2001) 213.
[10] Ph. Garcia, A. Bouloré, Y. Guérin, M. Trotabas, P. Goeuriot, P, in: Proceedings of the ANS (2000), Park City.

[11] L.H. Johnson, D.M. Leneveu, F. King, D.W. Shoesmith, M. Kolar, D.W Oscarson, S. Sunder, C. Onofrei, J.L. Crosthwaite, The disposal of Canada's nuclear fuel waste: a study of postclosure safety of in-room emplacement of used CANDU fuel in copper canisters in permeable plutonic rock, Volume 2: Vault model Atomic Energy of Canada Limited Report AECL-11494-2, COG-95-552-2 (1996).
[12] R.S. Forsyth, L.O. Werme, J. Nucl. Mater. 190 (1992) 3.
[13] R.S. Forsyth, The SKB Spent Fuel Corrosion Programme. An evaluation of results from the experimental programme performed in the Studsvik Hot Cell Laboratory, SKB Technical Report 97-25 (1997).
[14] W.J. Gray, in: D.J. Wronkewiecz, J.H. Lee (Eds.), Scientific Basis for Nuclear Waste Management XXII, Mater. Res. Soc. Symp. Proc. 556 (1999), p. 487.
[15] V.M. Oversby, H.F. Shaw, Spent fuel performance data: an analysis of data relevant to the NNWSI project, Lawrence Livermore National Laboratory Report UCID-20926 (1987).
[16] C.N. Wilson, in: M.J. Apted, R.E. Westerman (Eds.), Scientific Basis for Nuclear Waste Management XI, Mater. Res. Soc. Symp. Proc. 112 (1988), p. 473.
[17] C.N. Wilson, H.F. Shaw, in: J.D. Bates, W.B. Seefeldt (Eds.), Scientific Basis for Nuclear Waste Management X, Mater. Res. Soc. Symp. Proc. 84 (1987), p. 123.
[18] C.N. Wilson, W.J. Gray, Mater. Res. Soc. Symp. Proc. 176 (1990) 489.
[19] W.I. Neal, S.A. Rawson, W.M. Murphy, in: M.J. Apted, R.E. Westerman (Eds.), Scientific Basis for Nuclear Waste Management XI, Mater. Res. Soc. Symp. Proc. 112 (1988), p. 505.
[20] B. Grambow, A. Loida, A. Martinez-Esparza, P. Diaz-Arocas, J. De Pablo, J.-L. Paul, G. Marx, J.-P. Glatz, K. Lemmens, K. Ollila, H. Christensen, Source term for peformance assessment of spent fuel as a waste form. European Commission Report EUR 19140 EN (2000).
[21] L.H. Johnson, D.W. Shoesmith, in: W. Lutze, R.C. Ewing (Eds.), Radioactive Waste Forms for the Future, Elsevier, Amsterdam, 1988.
[22] D. Cubbicciotti, J.E. Sanecki, J. Nucl. Mater. 78 (1978) 96.
[23] W.H. Hocking, A.M. Duclos, L.H. Johnson, J. Nucl. Mater. 209 (1994) 1.
[24] C.N. Wilson, Results from cycles 1 and 2 of NNWSI series 2 spent fuel dissolution tests, HEDL-TME 85-22 UC-70 (1987), Westinghouse Hanford Company.
[25] P. Lovera, C. Ferry, C. Poinssot, L.H. Johnson, Synthesis report on the relevant diffusion coefficients of fission products and helium in spent nuclear fuels, CEA-Report CEA-R-6039 (2003).
[26] A.H. Booth, AECL Report CRDC-721 (1957).